END

FILMED

DTIC

1.0

4.5
5.0
5.6

2.8

2.5

3.2

2.2

3.6

4.0

2.0

1.1

1.8

1.25

1.4

1.6

MICROCOPY RESOLUTION TEST CHART
NATIONAL BUREAU OF STANDARDS-1963-A

| REPORT DOCUMENTATION PAGE | READ INSTRUCTIONS BEFORE COMPLETING FORM | |
|---|---|---|
| 1. REPORT NUMBER<br>AFGL-TR-82-0295 | 2. GOVT ACCESSION NO.<br>AD-A123 357 | 3. RECIPIENT'S CATALOG NUMBER |
| 4. TITLE (and Subtitle)<br>GRAVITY PARAMETER ESTIMATION FROM LARGE DATA SETS USING STABILIZED INTEGRAL FORMULAS AND A NUMERICAL INTEGRATION BASED ON DISCRETE POINT DATA | 5. TYPE OF REPORT & PERIOD COVERED<br>Scientific Report No. 2 | |
| | 6. PERFORMING ORG. REPORT NUMBER<br>Dept. of Geodetic Sci # 339 | |
| 7. AUTHOR(s)<br>Reiner Rummel | 8. CONTRACT OR GRANT NUMBER(s)<br>F19628-82-K-0022 | |
| 9. PERFORMING ORGANIZATION NAME AND ADDRESS<br>Dept. of Geodetic Science & Surveying<br>The Ohio State University--1958 Neil Avenue<br>Columbus, Ohio 43210 | 10. PROGRAM ELEMENT, PROJECT, TASK AREA & WORK UNIT NUMBERS<br>61102F<br>2309G1 BC | |
| 11. CONTROLLING OFFICE NAME AND ADDRESS<br>Air Force Geophysics Laboratory<br>Hanscom AFB, Massachusetts 01730        LWG<br>Scientific Program Officer--Dr. Christopher Jekeli | 12. REPORT DATE<br>September 1982 | |
| | 13. NUMBER OF PAGES<br>36 | |
| 14. MONITORING AGENCY NAME & ADDRESS(If different from Controlling Office) | 15. SECURITY CLASS. (of this report)<br>Unclassified | |
| | 15a. DECLASSIFICATION/DOWNGRADING SCHEDULE | |

16. DISTRIBUTION STATEMENT (of this Report)

Approved for public release; distribution unlimited

17. DISTRIBUTION STATEMENT (of the abstract entered in Block 20, if different from Report)

18. SUPPLEMENTARY NOTES

19. KEY WORDS (Continue on reverse side if necessary and identify by block number)

geodesy, gravity, estimation theory

20. ABSTRACT (Continue on reverse side if necessary and identify by block number)

A gravity parameter estimation technique is proposed that allows the processing of arbitrarily large and (at least locally) densely spaced, homogeneous sets of observations. The method is characterized by two independent features: First, for a problem at hand the least-squares collocation estimator is replaced by its corresponding global limit where it becomes a stable integral formula. This way the large (infinite dimensional) system of linear equations can be solved analytically. Moreover, since the integral formulas represents an optimal estimator a reliable error measure can be linked to it. Second, the

DD FORM 1473 1 JAN 73    EDITION OF 1 NOV 65 IS OBSOLETE

integral formula is approximated by numerical integration, but directly based on the discrete point observations instead of the commonly used mean block values. The required area weights attached to each observation are derived from a numerical triangulation spread over all data points. In a first and preliminary test some 1°x1° mean gravity anomalies were computed from GEOS-3 altimetry.

# Foreword

This report was prepared by Dr. Reiner Rummel of the Delft Univeristy of Technology. The initial studies described in this report were supported through Contract No. F19628-79-C-0027, Air Force Geophysics Laboratory, Hanscom Air Force Base, Massachusetts. The typing of this report was carried out under Contract No. F19628-82-K-0022.

Valuable discussions with O. Colombo, Stuttgart, M. Gerstl, Munchen, and R. H. Rapp, Columbus are gratefully acknowledged. The computer algorithm for the numerical triangulation in a plane was made available by M. Gerstl.

The reproduction and distribution of this report was carried out through funds supplied by the Department of Geodetic Science and Surveying. This report was also distributed by the Air Force Geophysics Laboratory as document AFGL-TR-82-0295, Scientific Report No. 2 under Contract F19628-82-K-0022.

Accession For

NTIS GRA&I

DTIC TAB

Unannounced

Justification

Distribution/

Availability Codes

Dist | Avail and/or Special

-iii-

## 1. Introduction

In practice gravity parameters, such as geoid heights, or deflections
of the vertical are derived either by numerical integration of one of the
well-known integral formulas of physical geodesy, or by an optimal estima-
tion technique such as least-squares collocation. In the frame of the
present days state-of-art--$10^{-6}$ to $10^{-7}$ relative precision, i.e. e.g.
geocentric distances to about 0.5 to 5 meters--both strategies yield reliable
results of sufficient accuracy. But in view of both, improving measurement
technology, and the availability of a rapidly increasing number of obser-
vations, one aims, mainly in the context of geodynamics, for $10^{-8}$ . This
high goal requires however not only improved functional models but at the
same time computation techniques that make adequate use of the physical
information contained in the large set of observations. And at this point
the individual limitations of these methods become visible.

So does the numerical integration approach not represent an estimation
technique. As a consequence there is no direct way to associate an error
measure to it. Further on, not the original (point) observations are used
for the integration process, but block mean values of a certain block size,
derived from them. But there exist many ways to compute mean values and
their standard deviations from the point observations. In addition, one
can hardly ever be sure that all mean values entering the numerical integra-
tion are derived by the same processing procedure.

Least squares collocation, on the other hand, does work with the original
point observations and is an optimal estimator. The well-known problem
is, however, that a system of linear equations has to be solved of a size
equal to the number of observations. Thus, as an inherent contradiction,
the more data are collected, or the smaller the sample intervals between
them, the more unstable the solution becomes, although a meaningful global
limit (for a globally continuous data coverage) exists. As a consequence,
one is restricted to comparably small data sets.

Strategies to overcome these deficiencies reach from (1) the arrange-
ment of the sample points in a regular pattern so as to produce certain

-1-

favorable matrix patterns, cf. (Colombo, 1979), via (2) sequential estimation combining potential coefficients, mean, and point values, cf. (Tscherning, 1975), to (3) e.g. a combined integral formula and collocation approach, as presented in (Lachapelle, (1977).

The method presented here tries to combine the strong points of the numerical integration and the least-squares collocation method, while avoiding their individual deficiences. It is based on the global limit of least-squares collocation--where an analytical inversion of the in-the-global limit infinite dimensional system of linear equations becomes possible-- and maintains therefore its character as an optimal estimator with an error measure associated to it. This global limit estimator can be expressed as a stabilized integral formula. A numerical integration applied to it allows to process arbitrarily large data sets. In deriving representative "area weights" it becomes possible to base the integration on the original point values.

The two essential features of the new method, the derivation of a global, stabilized estimator and the numerical integration based upon the original point observations, which complement each other in an ideal manner, are in principle independent. So could one apply any other numerical integration to the stabilized integral formula, too, e.g. the classical one using mean block values. On the other hand, there are many more applications of the numerical integration based on point values, than the one discussed in this context.

## 2. Stabilized Global Estimator

In (Neyman, 1974) and along a different line in (Moritz, 1975) a so-called "modified Stokes function" is derived:

$$SK(\psi_{PQ}) = R \sum_{\ell=2}^{\infty} \frac{2\ell+1}{\ell-1} \frac{c_\ell^g}{c_\ell^g + d_\ell} P_\ell(\cos\psi_{PQ}) \tag{1}$$

It differs from the Stokes kernel because of the filter factor

$$f_\ell = \frac{c_\ell^g}{c_\ell^g + d_\ell} . \tag{2}$$

-2-

In equation (1) it is

$P_{\ell}(\cos\psi_{PQ})$...Legendre polynomial of degree $\ell$ ,

$\psi_{PQ}$          ...spherical distance between $P$ and $Q$ ,

$c_{\ell}^{g}$          ...gravity anomaly model degree variance, and

$d_{\ell}$          ...a priori error degree variance.

We shall derive in the sequel this equation in detail for an arbitrary gravity estimation problem. Let us assume a set of $n$ observed ("~") gravity parameters, $\tilde{g}_i$ a given. As unknown the global disturbing potential function, $t$ , is chosen. Once an approximation of $t$ is derived, any other functional of it can be computed straightforwardly. The character of $t$ as a function shall be indicated by expressing it as a vector $\underline{t}$ of dimension ($\infty \times 1$). To be more precise, we assume $t \in H$ , a Hilbert space with reproducing kernel $K(P,Q) = C_{tt}(P,Q)$ . The spectral components or coefficients, $t_{\ell m}$ , of $t$ form an infinite but countable sequence, or vector of coefficients, $\varepsilon \ell_2$ isomorphic to $H$ , see e.g. (Meissl, 1976). It is

$$t(P) = \sum_{\ell=2}^{\infty} \sum_{m=-\ell}^{+\ell} \left(\frac{R}{r_p}\right)^{\ell+1} t_{\ell m} \bar{Y}_{\ell m}(P) , \qquad (3)$$

where $\bar{Y}_{\ell m}$ is a short-hand notation for the fully-normalized surface spherical harmonics of degree $\ell$ and order $m$

$$\bar{Y}_{\ell m}(P) = \begin{cases} \bar{P}_{\ell m}(\sin\phi_p) \cos m \lambda_p & \text{for } m \geq \ell \\ \bar{P}_{\ell|m|}(\sin\phi_p) \sin|m|\lambda_p & \text{for } m < \ell , \end{cases} \qquad (4)$$

$R$ is the radius of a convergence (Bjerhammar) sphere, and $r_p$ the geocentric radius of $P$ . For $K(P,Q)$ we choose, cf. (Moritz, 1980) the convergent series

$$K(P,Q) = C_{tt}(P,Q) = \sum_{\ell=0}^{\infty} \left(\frac{R^2}{r_p r_Q}\right)^{\ell+1} c_{\ell} P_{\ell}(\cos\psi_{PQ}) , \qquad (5)$$

with $c_{\ell}$ the disturbing potential degree variances. The functional relationship between the observable $g$ and $t$ may be described by the operator equation

$$\underline{g} = \underline{S}^{-1} \underline{t} . \qquad (6)$$

$n\times 1 \quad n\times\infty \quad \infty\times 1$

The corresponding relation between the spectral components may be written as

$$g_{\ell,m} = \lambda_\ell \; t_{\ell m} \; ,$$

with $\lambda_\ell$ only dependent on $\ell$ in case the operator $S^{-1}$ is isotropic, cf. (Neyman, 1974). For a detailed derivation in terms of an eigenvalue decomposition, see (Rummel et. al., 1979).

Example: In case $g$ is a vector of gravity anomalies, the functional is

$$g = - \left( \frac{2}{R} + \frac{\partial}{\partial r} \right) t \; ,$$

the so-called fundamental boundary condition of physical geodesy. Together with eq. (3) one obtains an expression of the type of eq. (6)

$$g(P) = \sum_{\ell m} \left( \frac{R}{r_p} \right)^{\ell+1} \frac{\ell-1}{r_p} \; \bar{t}_{\ell m} \; \bar{Y}_{\ell m}(P) \; .$$

The spectral components or eigenvalues of $S^{-1}$ are in this case

$$\lambda_\ell = \frac{\ell-1}{r_p}$$

$\square$

We assume $E\{\tilde{g}\} = g$ and $E\{(\tilde{g}-g)(\tilde{g}-g)^T\} = \underline{D}$. The least-squares collocation estimate, $\hat{t}$, ("^" estimated) is derived from the solution of the variational problem

$$\min \left( \| \tilde{g} - \underline{S}^{-1}\underline{t} \|^2_{\underline{D}^{-1}} + \alpha \| t \|^2_{\underline{C}_{tt}^{-1}} \right) \; , \quad \alpha > 1 \; , \tag{8}$$

cf. (Rummel et. al., 1979) or (Moritz, 1980, ch. 28). We obtain.

$$\underset{\infty \times 1}{\hat{t}} = (\underline{S}^{-T}\underline{D}^{-1}\underline{S}^{-1} + \alpha\underline{C}_{tt}^{-1})^{-1} \; \underline{S}^{-T}\underline{D}^{-1}\tilde{g}$$

$$= \underline{C}_{tt}\underline{S}^{-T} \; (\underline{S}^{-1}\underline{C}_{tt}\underline{S}^{-T} + \alpha\underline{D})^{-1} \; \tilde{g} \tag{9}$$

$$\underset{\infty \times \infty \;\; \infty \times n \;\; n \times \infty \;\; \infty \times \infty \;\; \infty \times n \;\; n \times n \;\; n \times 1}{}$$

The terms $\underline{C}\underline{S}^{-T}$ and $\underline{S}^{-1}\underline{C}\underline{S}^{-T}$ in (9) express the application of the operator $\underline{S}^{-1}$ to $\underline{C}_{tt}$, the well-known "propagation law of covariances". We write in short

$$\underset{\infty \times n}{C_{tg}} = \underline{C}_{tt}\, S^{-T}, \quad \text{and} \tag{10}$$

$$\underset{n \times n}{C_{gg}} = \underline{S}^{-1}\underline{C}_{tt}\underline{S}^{-T}. \tag{11}$$

We now consider the global limit of equation (9) where $\tilde{g}$ becomes a random function covering the entire surface of the earth or a sphere, e.g. in satellite altitude. A detailed derivation is given in the Appendix. If we denote the global limit of the linear estimator $\underline{C}_{tt}\underline{S}^{-T}(\underline{S}^{-1}\underline{C}_{tt}\underline{S}^{-T} + \alpha\underline{D})^{-1}$ by $L^T(P,Q)$ and the dimensionless filter or smoothing factor in eq. (A-14) by

$$f_\ell = \frac{(\frac{R}{r_Q})^{2(\ell+1)}\lambda_\ell^2 \bar{c}_\ell}{(\frac{R}{r_Q})^{2(\ell+1)}\lambda_\ell^2 \bar{c}_\ell + \alpha\sigma_0^2} = \frac{1}{1 + \frac{\alpha\sigma_0^2}{(\frac{R}{r_Q})^{2(\ell+1)}\lambda_\ell^2 \bar{c}_\ell}}, \tag{12}$$

We obtain from equation (A-14)

$$L(r_P, r_Q, \psi_{PQ}) = \sum_{\ell m} f_\ell \left(\frac{r_Q}{r_P}\right)^{\ell+1} \frac{1}{\lambda_\ell} \bar{Y}_{\ell m}(P)\, \bar{Y}_{\ell m}(Q)$$

$$= \sum_\ell f_\ell \left(\frac{r_Q}{r_P}\right)^{\ell+1} \frac{2\ell+1}{\lambda_\ell} P_\ell(\cos\psi_{PQ}). \tag{13}$$

For our example, with $\tilde{g}$ gravity anomalies, expression (13) becomes the modified Stokes function of equation (1). It would be identical to the classical Stokes function for $f_\ell = 1$. The global limit of the optimal estimator, equation (9), may now be written as

$$\hat{t}(P) = \lim_{Q_i \text{dense}} \{\underline{C}_{tg}(\underline{C}_{gg} + \alpha\underline{D})^{-1}\, \tilde{g}\}$$

$$= \underset{\infty \times \infty}{L^T}\, \underset{\infty \times 1}{\tilde{g}}$$

$$= \frac{1}{4\pi} \int_\sigma \left[\sum_\ell f_\ell \left(\frac{r_Q}{r_P}\right)^{\ell+1} \frac{2\ell+1}{\lambda_\ell} P_\ell(\cos\psi_{PQ})\right] \tilde{g}(Q)\, d\sigma_Q$$

$$= \frac{1}{4\pi} \int_\sigma L(r_P, r_Q, \psi_{PQ})\, \tilde{g}(Q)\, d\sigma_Q. \tag{14}$$

-5-

In (Rummel, 1982) it is shown that equation (14) may also be interpreted as an optimal solution of the stochastic variant of the global geodetic boundary value problem, with only one realization of $\tilde{g}$ given on the boundary surface.

The product $\lambda_\ell^2 \bar{\bar{c}}_\ell$ is the propagation of the disturbing potential degree variances to the degree variance of the observed gravity quantity. As to be seen from equation (12) and as discussed in (Gerstl & Rummel, 1981) the filter factors $f_\ell$ depend on
    -the a priori error variance $\sigma_0^2$ ,
    -the regularization factor $\alpha$ (usually chosen equal to 1),
    -the choice of the radius, R of the Bjerhammar sphere, and
    -the chosen degree variance model of t .
The stabilized integral kernel $L(r_P, r_Q, \psi_{PQ})$ can be cr structed very easily for any problem at hand, as long as g is a linear ft tion of t and exists even for cases where the non-stochastic counterpart do not. It is e.g. possible to construct a global "downward continuation" timator. Since, because of $\alpha\sigma_0^2$ , no closed formula can be found for ε on (13), it is in practice approximated by the Legendre polynomial truncated at a very high degree $\ell_{max}$ .

The next step shall be to prepare for a finite approximation of the stabilized global estimator from the discrete point observations. If one prefers to work instead with mean values of a certain block size, the traditional numerical integration techniques may be directly applied to equation (14).

## 3. Area Weights for Points Irregularly Distributed on a Sphere

The difficulty of performing a numerical integration directly based on point observations irregularly distributed on a sphere stems from the problem that area weights have to be assigned to the observations, that reflect the local data density. Area weight is thereby defined as a unique and representative surface area element (on the earth's surface, on a sphere, e.g. in satellite altitude, or simply on a unit sphere) assigned to an observed or derived gravity quantity value. When working with mean block values, they

are e.g. $\cos\phi\Delta\phi\Delta\lambda$ . Since the area weights have to reflect the local data density, i.e. small area weights for denser point samples, one has first to establish a quantitative relation between the points. One way to achieve this, is to connect the points by a triangular net with minimal side lengths and no side crossing another one, as displayed in Figure 1. Then one could compute the area of each triangle, e.g. MPQ, and associate to it the average of the observations $\tilde{g}_i$ at the three nodes. We shall follow another line: The areas of all triangles adjacent to one point, e.g. P , compare again Figure 1, are summed up and divided by three, because each triangle is shared by three points. It is the area weight $w_p$ , assigned to the discrete observation $\tilde{g}_p$ at P . The weights derived this way are unique, reflect the local data density, and their sum represents exactly the total area covered by the measurements. The result is a step function on the sphere (or the surface of the earth) with step area equal to $w_p$ and step size (height) equal to $\tilde{g}_p$ .
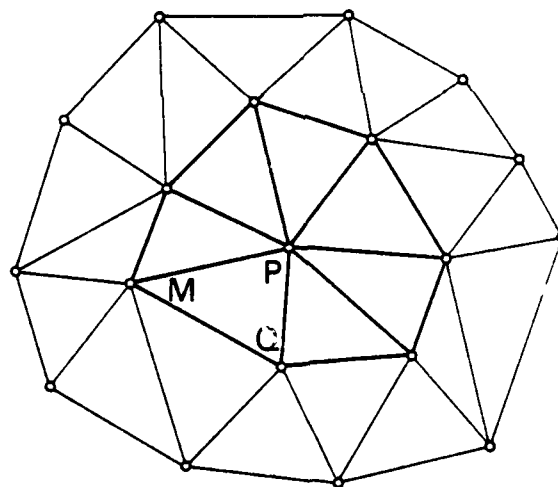


Figure 1

One could think of many sophistications of this principle. Instead of this discontinuous step configuration, continuous or continuously differentiable representations could be designed involving more and more of the neighboring observations for their definition. A consequence is a more complicated integration procedure.

The problem is now to find, first, the unique, minimum side lengths triangular net and, second, a fast algorithm for the computation of the area weights.

## 3.1  Closest Point Triangulation in a Plane

The problem of finding a unique, non-overlapping triangulation to irregularly distributed points , is well-covered in the literature, cf. (McCullagh & Ross, 1980) or (Peucker et. al., 1978). We shall base our computations on a computer algorithm developed by M. Gerstl, see (Gerstl et. al., 1979), that works in a plane. Its theoretical background is given in (Shamos & Hoey, 1975). The concept is as follows: Given is a list of Cartesian coordinates $x_i$ and $y_i$ of the points $Q_i$ . In a first step they have to be sorted such that $x_i < x_{i+1}$ and $y_i < y_{i+1}$ , if $x_i = x_{i+1}$ . Standard procedures performing the sorting are available at any computer installation. The first three points, $Q_1$ , $Q_2$ , and $Q_3$ of the sorted list form a triangle and the first stage of a convex hull that shall step by step be extended. $Q_4$ is connected with those vertices of the convex hull, it sees (two or three). Any side facing $Q_4$ has to be dropped if it can be intersected by a shorter one originating from $Q_4$ . The up-dated convex hull contains $Q_4$ . The same principle is now applied to every subsequent point of the sorted list. This way a triangulation is spread over all points, with no intersecting sides (except at the nodes $Q_i$) and with minimum side lengths. As a final product one obtains, first, a list counter-clockwise ordered of all points connected to each point and, second, an ordered list of all points of the final convex hull.

Modifications for the Work on a Sphere: The same principle could be directly employed to data given on a sphere, too. But in order to maintain

-8-

the efficiency of the fast computer algorithm in this case one has to avoid
the time-consuming trigonometric manipulations on the sphere as much as possible.
Therefore we compute beforehand from the given latitude, longitude, and radial
distance (or constant radius) 3-dimensional Cartesian coordinates of all points.
Side-length comparisons can then be based on chords instead of spherical dis-
tances. Azimuth comparisons, necessary for the decision which sides on the
convex hull are facing a new point, are carried out using $\phi$ and $\lambda$ as if
they were $x$ and $y$ because this approximation does not influence the compar-
ison.

## 3.2 Data Management Aspect

In principle the triangulation algorithm could be applied to data sets
of any size. But the program has to use an integer field LC(LMAX,NMAX) which
contains the ordered list of nodes joint to each point, with LMAX the total
number of points and NMAX the maximum number of joint points. Since the number
of joint points can run up to 50 very easily at an intermediate step of the
processing of a large point set, one arrives with point sets larger than
10,000 points easily at the storage limits of even very large computers. The
field dimension has to be kept so large because it is at least in theory pos-
sible that during the processing changes may occur even in the innermost zone
of the convex hull. We considered up to now three possibilities to circumvent
this problem:
1. One can store this field on external storage and work with direct access.
Then the computer program, which takes in its present form almost no c.p.u.-
time would loose much of its efficiency.
2. Another possibility is to process overlapping point sets independently and
afterwards merge them. Although this is not a very elegant method, it works
rather efficiently and has been applied for the numerical example following
below.
3. One could work with the maximum available storage and first build up a convex
hull in this limit. During the processing of subsequent points there exists
theoretically a chance that sides are changed in the inner zone of the convex

-9-

hull. But the chances are rather slim. Thus, one could simply freeze the inner
zone, i.e. not allow any changes, without hardly any loss in the criterion of
minimum side length. The frozen part could be stored externally and the cor-
responding core storage space recycled for further use. This possibility is
investigated at the moment.


## 3.3 Area Weight Computation

The area, $F$, of the sum of $m$ spherical triangles adjacent to a point
$P$, compare Figure 2, is:

$$F_p = \sum_{i=1}^{m} F_i = \frac{\pi}{180°} \sum_{i=1}^{m} \varepsilon_i , \qquad (15)$$

with $F_i$ area of the i-th spherical triangle and $\varepsilon_i = \alpha_i + \beta_i + \gamma_i - 180°$ ,
the corresponding spherical excess. It is then

$$F_p = \frac{\pi}{180°} [ \sum_i \alpha_i + \sum_i \beta_i + \sum_i \gamma_i ] - m \pi$$

or with $\kappa_i = \beta_i - \gamma_{i-1}$ and $\sum_i \alpha_i = 360°$

$$F_p = \frac{\pi}{180°} \sum_{i=1}^{m} \kappa_i - (m-2)\pi . \qquad (16)$$

The angles $\kappa_i$ are obtained from the spherical azimuths of the outside
edges. It is

$$\kappa_i = \begin{cases} -(A_{i,i+1} - A_{i,i-1}) & \text{if } \lambda_{i+1} > \lambda_i > \lambda_{i-1} \\ (A_{i,i+1} - A_{i,i-1}) & \text{otherwise.} \end{cases}$$

From $\tan A_{i,i+1}$ and $\tan A_{i,i-1}$ one computes $\tan \kappa_i$ by standard trigonometric
formulas. In order to avoid the evaluation of "arctan", one can use the recursion

$$\tan( \sum_{i=1}^{m} \kappa_i) = \frac{\tan(\sum_{i=1}^{m-1} \kappa_i) + \tan \kappa_m}{1 - (\tan \sum_{i=1}^{m-1} \kappa_i) \tan \kappa_m} \qquad (17)$$

for the computation of $\sum_{i=1}^{m} \kappa_i$ . Nevertheless, all spherical azimuths would have to be computed.

Again an approximation is introduced to avoid time-consuming spherical computations. Since dense data coverage is the underlying motivation for the whole method the type of approximation used here is justified. We use the Elling-formula, well-known from land surveying, and find, compare Figure 3:

$$F_p \doteq \tfrac{1}{2} \cos\phi_p \sum_{i=1}^{m} (\phi_i - \phi_{i+1})(\lambda_i + \lambda_{i+1})(\tfrac{\pi}{180°})^2 \ , \tag{18}$$

where $\cos\phi_p$ takes care of the convergence of the meridians. For a block enclosed by two latitude circles and two meridians, eq. (18) yields the usual area element $\cos\phi_p \Delta\phi \Delta\lambda$. No trigonometric function have to be computed when using eq. (18). Since each triangle is shared by three points, we finally find for the area weight

$$w_p = \tfrac{1}{3} F_p = \tfrac{1}{6}\cos\phi_p \sum_{i=1}^{m} (\phi_i - \phi_{i+1})(\lambda_i + \lambda_{i+1})(\tfrac{\pi}{180°})^2 \ . \tag{19}$$
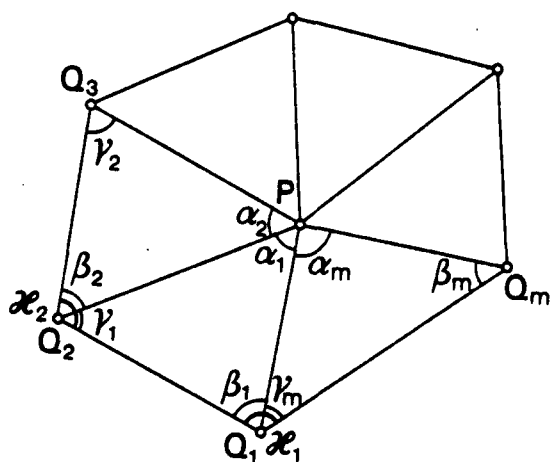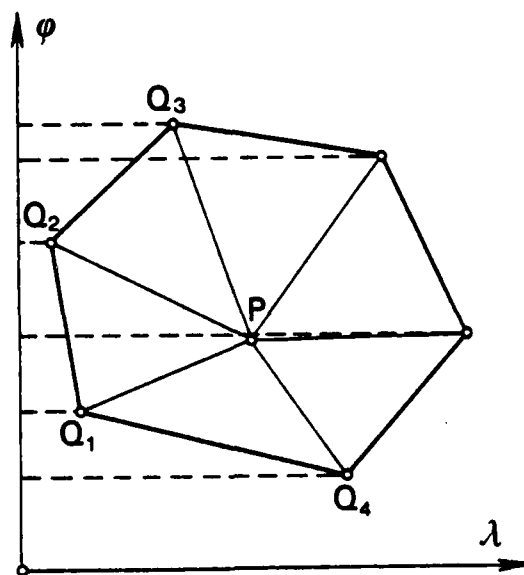


Figure 2



Figure 3

-11-

## 3.4 Final Data Base

After having carried out these computations the data base contains besides the original entities, e.g. point number, coordinates, measurement value, the computed area weight $w_p$. In addition, one can add a pointer to a separate data file, that contains a list of the adjacent nodes to each point, if needed for other applications. The points on the convex hull and their (distorted) area weights are not elements of the data base. They as well as their adjacent points should be stored in a separate data file. This way it is possible to restart at a later time the triangulation of a new area leaving the old data base unchanged.

New discrete points inside the original point set, e.g. new measurements $\tilde{g}$, can be incorporated in such a way that only that triangle is affected in which the new point is contained, (compare Figure 4). This way only four area weights, that of the incoming point and those of the three vertices of the triangle, have to be up-dated, on the expense that locally the minimum side length criterion is probably violated.
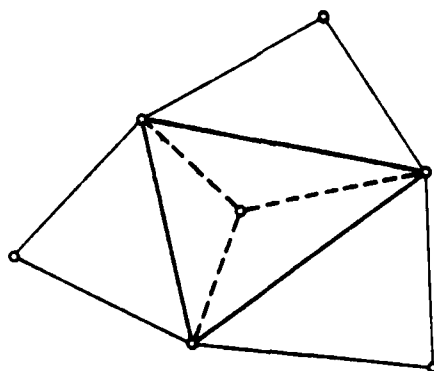


Figure 4

The here proposed philosophy of working with the point observations which are related through a "triangulation" with the points in their proximity is supported by a general trend. The availability of very powerful data management systems stimulates to work with the large sets of original observations and could make mean block averages more and more superfluous.

Many applications in geodesy, geophysics, surveying and civil engineering can be envisioned, such as
- the computation of gravity parameters, such as height anomalies, deflections of the vertical etc. from large sets of observations,
- the estimation of surface gravity parameters from satellite gravity sensors (gradiometry or satellite-to-satellite tracking),
- topographic or topographic-isostatic reduction and inverse geophysical modelling from digital terrain models, or
- height interpolation, mass-volume estimation, profile computation etc. from photogrammetric or tachymetric digital terrain models.

## 4. Error Estimate

As important as the estimate $\hat{t}$ itself is, we must have a reliable error measure for it. For a moment, we still remain with the global limit case, where $\tilde{g}$ is assumed to be a random function. The posteriori variance-covariance matrix of $\hat{t}$ eq. (9), resulting from least-squares collocation is, cf. (Moritz,1980):

$$\underline{E}_{tt} = \underline{C}_{tt} - \underline{C}_{tt}\underline{S}^{-T} (\underline{S}^{-1}\underline{C}_{tt}\underline{S}^{-T} + \alpha\underline{D})^{-1} \underline{S}^{-1} \underline{C}_{tt} \qquad (20)$$

$$\infty\times\infty \quad \infty\times\infty \quad \infty\times\infty\infty\times n \quad \infty n\times\infty \infty\times\infty \infty\times n \quad n\times n \quad n\times\infty \infty\times\infty$$

-13-

or with the defined linear estimator, eq. (13),

$$\underline{E}_{tt} = \underline{C}_{tt} - \underline{L}^T \underline{S}^{-1} \underline{C}_{tt} \cdot \qquad (21)$$

$$\infty\times\infty \qquad \infty\times\infty \quad \infty\times n \quad n\times\infty \quad \infty\times\infty$$

From a simple manipulation we obtain

$$\underline{E}_{tt} = \underline{C}_{tt} - \underline{L}^T \{(\underline{S}^{-1} \underline{C}_{tt} \underline{S}^{-T} + \alpha\underline{D}) (\underline{S}^{-1} \underline{C}_{tt} \underline{S}^{-T} + \alpha\underline{D})^{-1}\} \cdot$$

$$\cdot \underline{S}^{-1} \underline{C}_{tt} =$$

$$= \underline{C}_{tt} - \underline{L}^T (\underline{S}^{-1} \underline{C}_{tt} \underline{S}^{-T} + \alpha\underline{D}) \underline{L} \qquad (22)$$

Furtheron with a similar manipulation one derives from equation (20):

$$\underline{E}_{tt} = \underline{C}_{tt} - \underline{C}_{tt} \underline{S}^{-T} \underline{L} - \underline{L}^T \underline{S}^{-1}\underline{C}_{tt} + \underline{L}^T(\underline{S}^{-1}\underline{C}_{tt} \underline{S}^{-T} + \alpha\underline{D}) \underline{L}$$

$$= (\underline{L}^T\underline{S}^{-1} - \underline{I})\underline{C}_{tt} (\underline{L}^T\underline{S}^{-1}-\underline{I})^T + \alpha\underline{L}^T\underline{D}\underline{L}$$

$$= \underline{B}^T\underline{C}_{tt}\underline{B} + \alpha\underline{L}^T \underline{D} \underline{L} \qquad (23)$$

$$\infty\times\infty \quad \infty\times\infty \quad \infty\times\infty \quad \infty\times n \quad n\times n \quad n\times\infty$$

with the unit matrix $\underline{I}$ and the bias expression

$$\underline{B}^T = \underline{I} - \underline{L}^T \underline{S}^{-1} \qquad (24)$$

$$\infty\times\infty \quad \infty\times\infty \quad \infty\times n \quad n\times\infty$$

Equations (21), (22), and (23) are three alternative forms to equation (20). Equation (22) is convenient from the numerical evaluation point of view, because the inversion of the full matrix $(\underline{S}^{-1}\underline{C}_{tt}\underline{S}^{-T}+\alpha\underline{D})$ is avoided, once $\underline{L}$ is known. Equation (23) is interesting from the interpretation point of view. Equations (20) to (24) are still infinite dimensional. For the evaluation of the a posteriori variance $m_P^2$ at $P$, (or analogously, the covariance between two arbitrary points $P$ and $Q$) it is convenient to introduce the evaluation functional $\underline{e}_P^T$. We define e.g.

$$\underline{L}_P^T \stackrel{\text{def.}}{=} \underline{e}_P^T \underline{L}^T \cdot \qquad (25)$$

$$1\times n \qquad 1\times\infty \quad \infty\times n$$

-14-

Then equations (22) and (23) become

$$m_P^2 = C_{tt,P} - \underline{L}_P^T (\underline{S}^{-1}\underline{C}_{tt}\underline{S}^{-T} + \alpha\underline{D}) \underline{L}_P$$

$$= C_{tt,P} - \underline{L}_P^T (\underline{C}_{gg} + \alpha\underline{D}) \underline{L}_P \tag{26}$$

and

$$m_P^2 = \underline{B}_P^T \underline{C}_{tt} \underline{B}_P + \alpha\underline{L}_P^T \underline{D} \underline{L}_P . \tag{27}$$

With equations (A-3) and (A-14) of the appendix we find for the spectral form of equation (26):

$$m_P^2 = \sum_\ell (\frac{R}{r_P})^{2(\ell+1)} (2\ell + 1) \bar{\bar{c}}_\ell -$$

$$- \sum_\ell f_\ell^2 (\frac{r_Q}{r_P})^{2(\ell+1)} \frac{1}{\lambda_\ell^2} ((\frac{R}{r_Q})^{2(\ell+1)}\lambda_\ell^2 \bar{\bar{c}}_\ell + \alpha\sigma_\delta^2) (2\ell+1)$$

$$= \sum_\ell (\frac{R}{r_P})^{2(\ell+1)} c_\ell -$$

$$- \sum_\ell (\frac{R}{r_P})^{2(\ell+1)} c_\ell f_\ell =$$

$$= \sum_\ell (\frac{R}{r_P})^{2(\ell+1)} c_\ell(1 - f_\ell) , \tag{28}$$

where we used that $\sum_m \bar{Y}_{\ell m}(P) \bar{Y}_{\ell m}(P) = (2\ell+1) P_\ell(1) = 2\ell+1$ . From equation (12) one obtains for

$$(1 - f_\ell) = \frac{\alpha\sigma_\delta^2}{(\frac{R}{r_Q})^{2(\ell+1)}\lambda_\ell^2 \bar{c}_\ell + \alpha\sigma_\delta^2} \tag{29}$$

Together with eq. (28) it yields the limits

$$\lim_{\sigma_\delta^2 \to 0} m_P^2 = 0$$

and

$$\lim_{\sigma_\delta^2 \to \infty} m_P^2 = \sum_\infty (\frac{R}{r_P})^{2(\ell+1)} c_\ell = C_{tt,P} ,$$

i.e. the a posteri variance becomes equal to the a priori one. All these error estimates hold for the case where a global random function $\tilde{g}$ is assumed to be given. In reality we assume densely spaced point observations $\tilde{g}_i$ , i=1,...n . Equation (14) is approximated by a numerical integration procedure. Equation (14)

$$\hat{t}_p = \frac{1}{4\pi} \int_\sigma L(r_p, r_Q, \psi_{PQ}) \, \tilde{g}(Q) \, d\sigma_Q$$

$$= \underset{1 \times \infty \quad \infty \times 1}{\underline{L}_p^T \, \tilde{\underline{g}}}$$

is replaced with very little loss by

$$\hat{t}_p \triangleq \sum_{i=1}^n L'(r_p, r_{Q_i}, \psi_{PQ_i}) \, \tilde{g}_i \, \frac{w_i}{4\pi} \quad . \tag{30}$$

In equation (30) the $w_i$ are the area weights as obtained from eq. (19), and $L'$ is the discrete approximation of the operator $L$, eq. (13). Important is thereby that for the computation of $L'$, $\sigma_0^2$ has to be replaced by

$$d' = \frac{\Delta s}{4\pi} \, \sigma_0^2 \tag{A-10}$$

with $\Delta s = \frac{1}{n} \sum_{i=1}^n w_i$, the average area weight. Thus, the a posteriori variance, equation (27), becomes

$$m_p^2 = \underline{B}_p'^T \, \underline{C}_{tt} \, \underline{B}_p' + \alpha \underline{L}_p'^T \, \underline{D} \, \underline{L}_p' \tag{31}$$

i.e. in all expressions $L$ is replaced by $L'$ ($\alpha$ is usually chosen $\alpha \overset{def}{=} 1$). The second term on the right-hand side of equation (31) becomes for uncorrelated observations with homogeneous a priori variance

$\sigma_0^2 \, \underline{L}_p'^T \, \underline{L}_p' \ldots$ the <u>pure error propagation</u>. This is the only part usually considered in geodetic numerical integration procedures. It is also well-known from the least-squares adjustment of overdetermined problems. As important is the first term

$\underline{B}_p'^T \, \underline{C}_{tt} \, \underline{B}_p' \ldots$ the <u>discretisation error.</u> From the definition of $\underline{B}$, equation (24), one sees that this part becomes zero for global and continuous data, free of errors. For a large amount of observations, its evaluation is rather tedious, because of the size of $\underline{C}_{tt}$.

## 5. Numerical Example

In a first and still preliminary test the method was tested through a computation of some 1°x1° mean gravity anomalies from adjusted GEOS-3 altimeter data in the North Atlantic. This example was chosen for several reasons:

- The GEOS-3 altimeter data fulfills very well the requirement of being at least locally dense and homogeneous.
- The computation of gravity anomalies from the "quasi" geoid undulations as obtained from altimetry, poses a very unstable problem. Thus, it is a good test for the stability behavior of this numerical integration approach.
- In the same geographical area 1°x1° anomalies are available as obtained from shipborne gravity measurements, as well as those estimated from GEOS-3 altimetry by least-squares collocation, compare (Rapp, 1977). With collocation typically around 400 observations could be processed per gravity anomaly estimate out of the total number of 500,000, whereas with the new method we could easily work with 7000 without even taking into account the data management aspects mentioned in Chapter 3.2.

In this test computation approximately 7000 adjusted sea surface heights as derived from GEOS-3 altimetry were included. At the accuracy level of GEOS-3 ($\pm 0.5$ to $0.8$ m) they can be considered synonymous to geoid undulations. The adjustment of the altimeter data is described in (ibid.). The processing steps of the new method are displayed in a flow chart in Figure 5. First, for all points the area weights were computed according to eq. (19) and included in the data file. Prerequirement was the determination of a triangulation connecting all points, as described in Chapter 3.1 The triangle net is shown in Figure 6, where one can still recognize the original pattern of the satellite ground tracks. In an enlarged sub-area the principle of the area weight computation is illustrated, Figure 7. Independent thereof, a table with the function values of the stabilitzed integral kernel, equation (13), was computed at small intervals $\Delta \psi = 1'$, i.e. at $\{\psi_k \mid 0° (1') 15°\}$. During the numerical integration process it is linearily interpolated between the tabulated values. The computation of the table values, theoretically a summation up to infinity, has been truncated at $\ell_{max} = 10,000$. The degree variance model by Tscherning and Rapp (1974) was chosen for the definition of the $\bar{c}_\ell$, compare again eq. (13).

For the a priori error variance, $\sigma_\delta^2$ , we chose 0.64 $m^2$ (std. dev. ±0.8 m).
According to equation (A-10) $\sigma_\delta^2$ was multiplied by $\frac{\Delta s}{4\pi}$, with $\Delta s$ the average
area weight. The obtained d' is used instead of $\alpha\sigma_\delta^2$ in eq. (12). The tab-
ulated kernel values together with the area weights and the altimeter derived
geoid undulations allow to perform the numerical integration, equation (30),
completely along the line of e.g. the numerical integration of the Stokes' inte-
gral in the context of geoid computations. The long-wavelength part of the
undulations and of the mean gravity anomalies to be estimated has been treated
separately by subtracting from the altimeter derived undulations the contri-
butions coming from a set of potential coefficients and adding back the cor-
responding contribution to the mean anomalies. For the long-wavelength part
the Goddard Earth Model 9 set of potential coefficients up to degree 20 has been
used. Consequently the summation of the stabilized integral kernel, eq. (13),
has been started at degree 21. Table 1 shows the results for a set of arbitarily
selected 1°x 1° blocks. Column three gives the mean anomaly values as obtained
from the GEM-9 model, column four the terrestrial (shipborne gravimetry) mean
anomalies, column five the values obtained with the new method, column six the
collocation results provided by Dr. Rapp. The estimates derived with the new
approach show a good agreement with the terrestrial and collocation data with
an overall tendency to be closer to the terrestrial anomalies. It would be
unreasonable to draw any further reaching conclusions from this limited test.
This application can be considered an alternative to the techniques described
in (Rummel et. al., 1977).

| φ | λ | GEM-9 | terr. Δg | new method | l.s. collocation |
|---|---|---|---|---|---|
| 1 | 2 | 3 | 4 | 5 | 6 |
| 39 | 292 | -16.6 | -35 | -34.7 | -37.7 |
| 39 | 293 | -16.4 | -27 | -38.7 | -37.6 |
| 38 | 292 | -18.0 | -33 | -32.4 | -32.7 |
| 38 | 293 | -17.7 | -23 | -26.6 | -25.6 |
| 37 | 294 | -18.8 | -16 | -18.8 | -9.9 |
| 37 | 295 | -17.9 | -20 | -22.4 | -13.8 |
| 37 | 296 | -17.0 | -20 | -21.7 | -14.5 |
| 37 | 297 | -16.1 | -27 | -26.3 | -17.3 |

Table 1: A comparison of 1°x1° mean gravity anomalies estimated from geoid undulations (derived from GEOS-3 altimetry) by least squares collocation (column 6) and by the new technique (5) with the corresponding terrestrial values (4). The mean anomalies as obtained from the GEM-9 set of potential coefficients up to $\ell=20$ is contained in column 3. The coordinates φ and λ of the north-west corner of each block are given in columns 1 and 2. (Dimension Δg: mgal = $10^{-5}$ ms$^{-2}$)

## 6. Further Sophistications

One of the most important features of least-squares collocation is, that it allows to combine in an optimal way <u>heterogeneous data</u>, i.e. different gravity quantities distributed in an arbitrary manner over various points. Since the present method is derived from a global limit process, this feature is lost in this generality. With other words, there is no simple way to combine a gravity anomaly at one point with a deflection of the vertical component at another one, and a potential difference at a third point. Sjöberg (1979) has shown, however, that it is possible to combine heterogeneous data in the global limit, i.e. it is again possible to derive a global limit estimator analogous to chapter
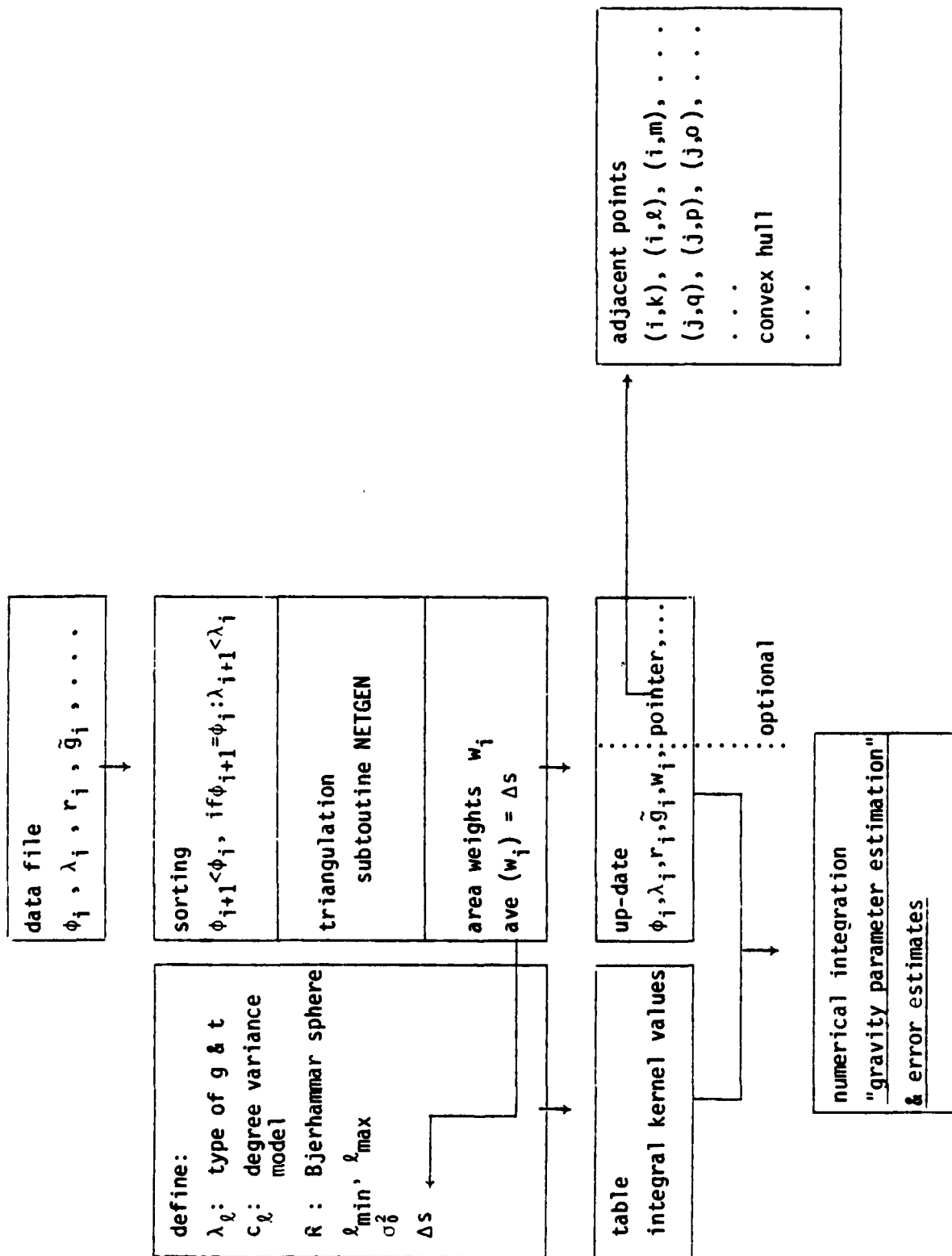
data file
$\phi_i, \lambda_i, r_i, \tilde{g}_i \ldots \ldots$

sorting
$\phi_{i+1} < \phi_i$, if $\phi_{i+1} = \phi_i : \lambda_{i+1} < \lambda_i$

triangulation
subroutine NETGEN

area weights $w_i$
ave $(w_i) = \Delta s$

define:
$\lambda_\ell$: type of g & t
$c_\ell$: degree variance model
$\bar{R}$ : Bjerhammar sphere
$\ell_{min}, \ell_{max}$
$\sigma_0^2$
$\Delta s$

up-date
$\phi_i, \lambda_i, r_i, \tilde{g}_i, w_i,$ pointer, ....

optional

adjacent points
$(i,k), (i,\ell), (i,m), \ldots$
$(j,q), (j,p), (j,o), \ldots$
$\ldots$
convex hull
$\ldots$

table
integral kernel values

numerical integration
"gravity parameter estimation"
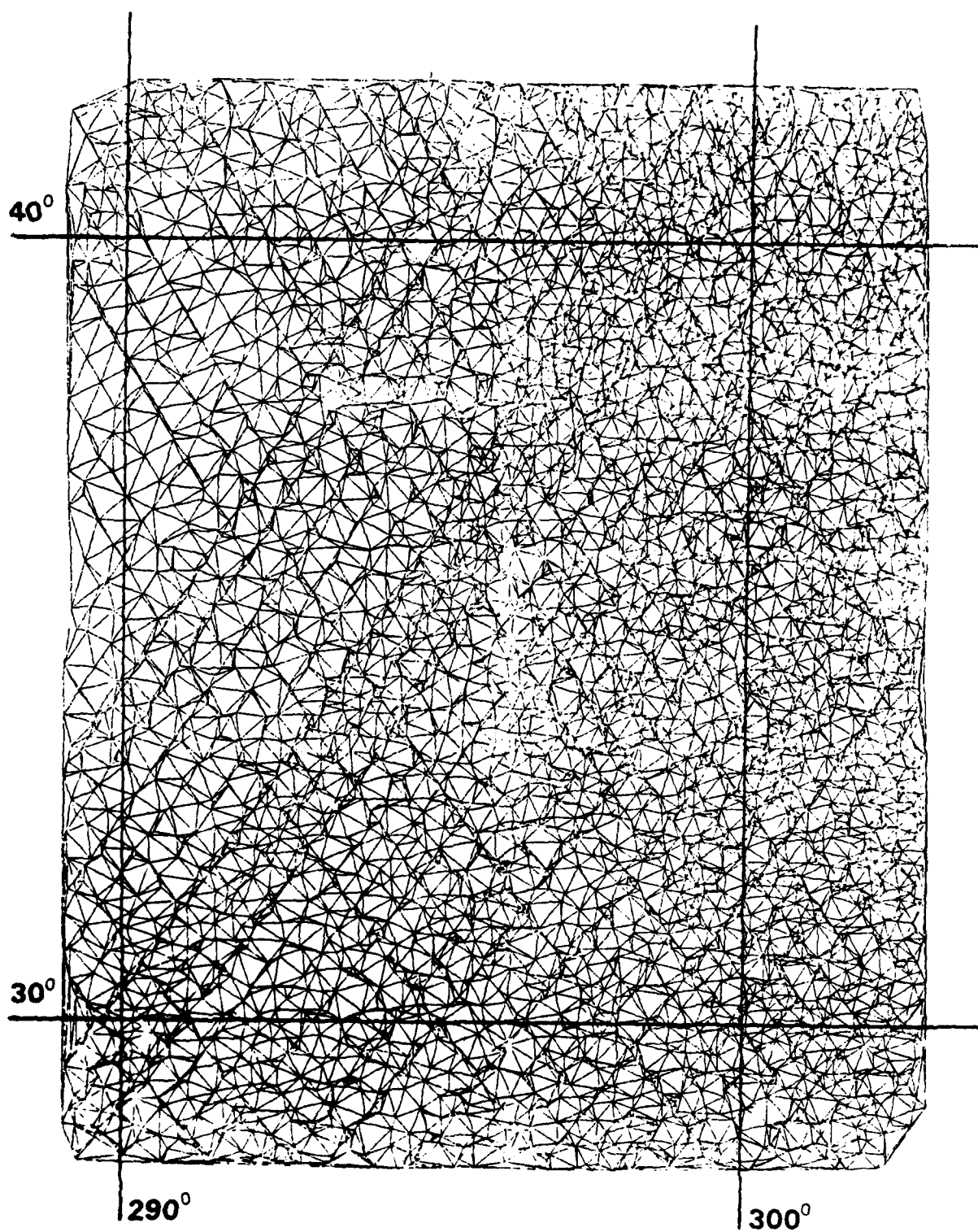& error estimates

Figure 5: Computational Scheme

-20-

**Figure 6:** Triangle net with minimum side lengths connecting approximately 7000 observation points of the GEOS-3 altimeter in the North Atlantic.
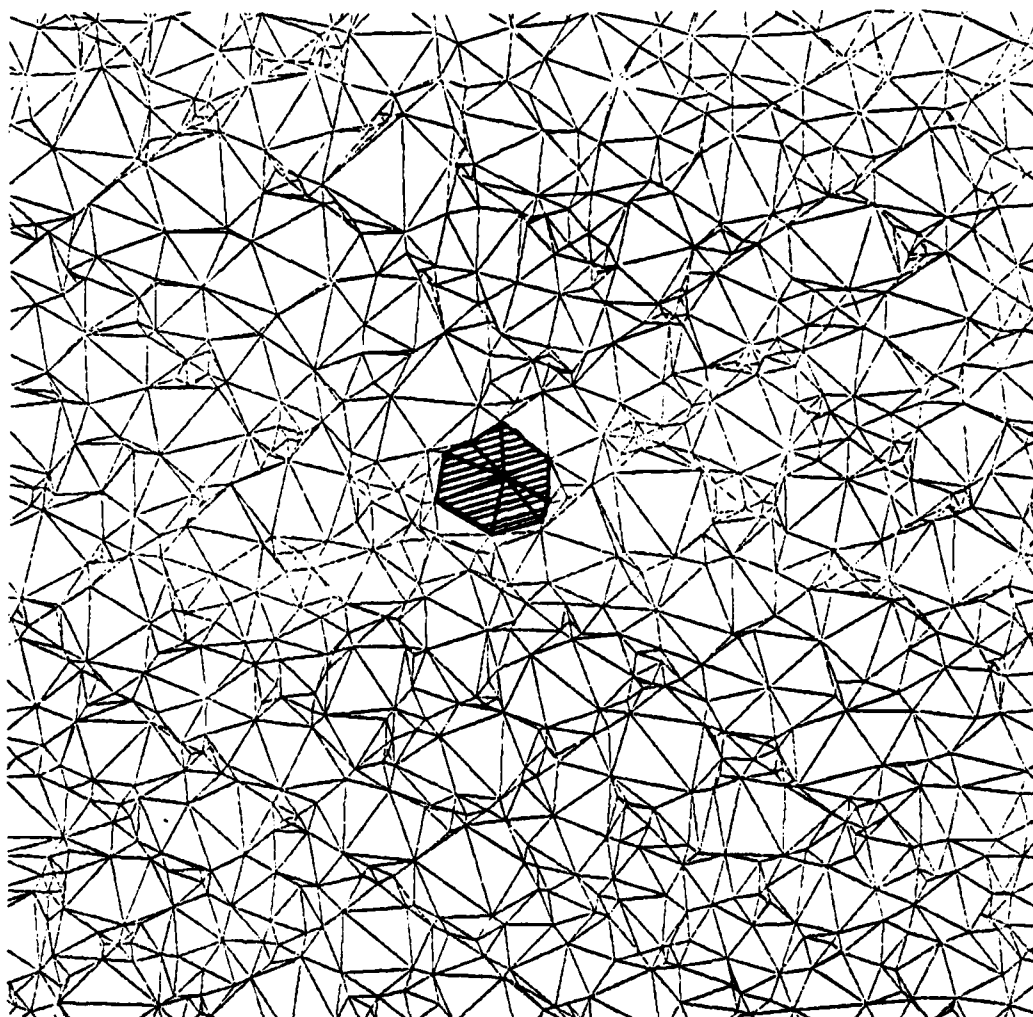
-21-

Figure 7: A portion of Figure 6 illustrating the computaiion of the area weights, which are defined as one third of the sum of areas over the triangles adjacent to each observation point.

2, that combines global random functions of different type. In its most general form the optimal estimator may be written, analogous to eq. (14), as:

$$\hat{t}(P) = \frac{1}{4\pi} \int_\sigma \underset{1 \times m}{\mathscr{L}}(r_P, r_Q, \psi_{PQ}) \begin{pmatrix} \tilde{g}^{(1)}(Q) \\ \tilde{g}^{(2)}(Q) \\ \vdots \\ \tilde{g}^{(m)}(Q) \end{pmatrix} d\sigma_Q \tag{32}$$

with $m$ different gravity quantities $\tilde{g}^{(j)}$, $j=1,\ldots m$. The expression for the vector estimator becomes, analogous to eq. (13):

$$\underset{1 \times m}{\mathscr{L}}(r_P, r_Q, \psi_{PQ}) = \sum_\ell \underset{1 \times m}{\mathbf{f}_\ell} \underset{m \times m}{\Lambda_\ell} \left(\frac{r_Q}{r_P}\right)^{2\ell+1} (2\ell+1) P_\ell(\cos\psi_{PQ}) \tag{33}$$

In eq. (33) $\underline{\Lambda}_\ell$ is the diagonal matrix

$$\Lambda_\ell = \begin{bmatrix} \frac{1}{\lambda_\ell^{(1)}} & & & 0 \\ & \frac{1}{\lambda_\ell^{(2)}} & \ddots & \\ & & & \\ 0 & & & \frac{1}{\lambda_\ell^{(m)}} \end{bmatrix}, \tag{34}$$

where the $\lambda_\ell^{(j)}$, $j=1,\ldots m$ are the spectral coefficients relating the observable quantities $g^{(j)}(Q)$ to $t(P)$, compare eq. (7). The dimensionless filter vector $\underset{\ell}{\mathbf{f}}$ becomes, analogous to eq. (12):

$$\mathbf{f}_\ell = \begin{bmatrix} \lambda_\ell^{(1)2} \\ \lambda_\ell^{(2)2} \\ \vdots \\ \vdots \\ \lambda_\ell^{(m)2} \end{bmatrix}^T \begin{bmatrix} \lambda_\ell^{(1)2} + \frac{\sigma_0^{(1)2}}{s^{\ell+1}\bar{c}_\ell} & \lambda_\ell^{(1)}\lambda_\ell^{(2)} & \cdots & \lambda_\ell^{(1)}\lambda_\ell^{(m)} \\ \lambda_\ell^{(2)}\lambda_\ell^{(1)} & \lambda_\ell^{(2)2} + \frac{\sigma_0^{(2)2}}{s^{\ell+1}\bar{c}_\ell} & \cdots & \lambda_\ell^{(2)}\lambda_\ell^{(m)} \\ \vdots & \vdots & & \vdots \\ \lambda_\ell^{(m)}\lambda_\ell^{(1)} & \cdots & & \lambda_\ell^{(m)2} + \frac{\sigma_0^{(m)2}}{s^{\ell+1}\bar{c}_\ell} \end{bmatrix}^{-1}$$

where $s = \left(\frac{R}{r_Q}\right)^2$ and all regularization factors $\alpha^{(1)},\ldots\alpha^{(m)}$ were chosen equal to one. For the case of only two different observed gravity quantiites, $\tilde{g}^{(1)}$ and $\tilde{g}_Q^{(2)}$, the inversion contained in eq. (35) can be performed explicitly. We find after inversion ($\Delta$...determinant of the matrix):

$$
\mathfrak{F}_\ell = \begin{bmatrix} \lambda_\ell^{(1)} \\ \lambda_\ell^{(2)2} \end{bmatrix}^T \begin{bmatrix} \bar\lambda_\ell^{(2)2} + \dfrac{\sigma_0^{(2)2}}{s^{\ell+1}\bar{\bar{c}}_\ell} & -\lambda_\ell^{(1)}\lambda_\ell^{(2)} \\ -\lambda_\ell^{(1)2}\lambda_\ell^{(2)2} & \lambda_\ell^{(1)2} + \dfrac{\sigma_0^{(2)2}}{s^{\ell+1}\bar{\bar{c}}_\ell} \end{bmatrix} \Delta^{-1} =
$$

$$
= \begin{bmatrix} \dfrac{1}{1 + \dfrac{\lambda_\ell^{(2)2}\bar{\bar{c}}_\ell\sigma_0^{(1)2} + \sigma_0^{(1)2}\,\sigma_0^{(2)2}}{\lambda_\ell^{(1)2}\bar{\bar{c}}_\ell\,\sigma_0^{(2)2}}} \\[3em] \dfrac{1}{1 + \dfrac{\lambda_\ell^{(1)2}\bar{\bar{c}}_\ell\sigma_0^{(2)2} + \sigma_0^{(1)2}\,\sigma_0^{(2)2}}{\lambda_\ell^{(2)2}\bar{\bar{c}}_\ell\,\sigma_0^{(1)2}}} \end{bmatrix} \qquad\qquad (36)
$$

Equations (32) to (35) are of practical relevance in cases where the same combination of gravity quantities is available in all of the densely spaced but discrete sampling points. Again the same numerical integration procedure can be employed. A typical example would be a satellite gradiometer mission, where in an ideal case in each sampling point five linearly independent second-order derivative components of the gravitational potential are observable. The benefit of having per point five components instead of only one can easily be investigated with the formula apparatus presented here.

The new method should permit a better exploitation of the information content of large and densely spaced sets of observed gravity quantities, prerequirement for a step towards a $10^{-8}$ relative accuracy. We did not at all go into the question what model improvements are required at the same time to achieve this goal. But since the new method is set up the same way as the classical numerical integration techniques in physical geodesy, all model sophistications developed for them can be applied here, too. This includes especially ellipsoidal correction, and tidal, topographic and ellipsoidal reduction, as discussed in the literature, cf. (Mather, 1973), (Moritz, 1974), (Rummel & Rapp, 1976), (Rapp, 1981), (Groten, 1982), although on the other hand the reduction concept is not very attractive from the theoretical point of view, and should eventually be replaced by more sophisticated models. Also the numerical side can be improved, e.g. by minimizing the truncation error, when working with data limited to a certain cap, compare (Jekeli, 1980), or by optimizing the combination with sets of potential coefficients, as proposed by Wenzel (1981).

## 7. Conclusions

From the application point of view, the classical numerical integration
procedures in physical geodesy have two disadvantages. They are not estimators
and are therefore not linked to a stochastic model and they work with mean block
values, which come from some subjectively chosen pre-processing. Linear estima-
tion techniques, such as least-squares collocation, on the other hand, who do
not have these drawbacks, require usually the solution of a large system of
linear equations, which limits their applicability. The technique presented
here tries to avoid these problems. It represents a "global limit" estimator.
Especially when treating unstable problems this offers considerable advantages
against the classical integral procedures. In addition, the error measure does
not contain only the pure error propagation, but also the discretisation error.
Independent of these features the numerical integration is based on discrete point
values. We hope to initiate a trend in this direction, which seems to us timely,
considering the fantastic prospects of modern data management capabilities. The
efficient processing of even very large sets of original observations should be
no problem in the near future. The numerical integration method itself, and
the underlying triangulation of "digital terrain model" type of data sets offers
many more applications than the one presented in our example, in geodesy, as well
as in surveying, photogrammetry, civil engineering, and geophysics. Examples
and envisioned improvements to be implemented in the numerical procedure are
lined out in Chapter 3.

The also described capability of optimal data combination based on the
ideas of L. Sjöberg, could be especially useful for the study of future dedicated
satellite gravity missions, to get an insight into the improvements coming from
simultaneously sensing the gravity field in different spatial directions.

Necessary model improvements, on the one hand, and optimal data processing,
on the other hand, seem to us the major obstacles on the way to a "$10^{-8}$-precise
gravimetric geodesy". This study is supposed to be a contribution to the latter.

## References

Colombo, O., Optimal Estimation from Discrete Data Regularly Sampled on a
Sphere, Dept. of Geodetic Science Report No. 291, The Ohio State University,
Columbus, 1979.

Gerstl, M., G. Heindl, E. Reinhart, Interpolation and Approximation by Piecewise
Quadratic Smooth Functions of Two Variables, paper presented at the 17th
IUGG General Assembly, Canberra, 1979.

Gerstl, M., R. Rummel, Stability Investigations of Various Representations
of the Gravity Field, Reviews of Geophysics and Space Physics, 19, 3, 415-
420, 1981.

Groten, E., A Precise Definition and Implementation of the Geoid and Related
Problems, Zeischrift für Vermessungsvesen, 1, 107, 26-32, 1982.

Heiskanen, W.A., H. Moritz, Physical Geodesy, Freeman & Co., San Francisco,
1967.

Jekeli, C., R. H. Rapp, Accuracy of the Determination of Mean Anomalies and
Mean Geoid Undulations from a Satellite Gravity Field Mission, Dept. of
Geodetic Science Report No. 307, The Ohio State University, Columbus, 1980.

Jekeli, C., Reducing the Error of Geoid Undulation Computations by Modifying
the Stokes' Function, Dept. of Geodetic Science Report No. 307, The Ohio
State University, Columbus, 1980.

Lachapelle, G., Estimation of Disturbing Potential Components Using a Combined
Integral Formula and Collocation Approach, Manuscripta Geodaetica, 2,4,
233-262, 1977.

Mather, R., A Solution of the Geodetic Boundary Value Problem to Order $e^3$ ,
Report X-592-73-11, NASA Goddard Space Flight Center, Greenbelt, 1973.

McCullagh, M.J., C.G. Ross, Delaunay Triangulation of a Random Data Set for Isarithmic Mapping, Cartographic Journal, 17, 2, 93-99, 1980.

Meissl, P., Hilbert Spaces and their Application to Geodetic Least Squares Problems, Bolletino de Geodesia e Scienze Affini, 35, 1, 49-80, 1976.

Moritz, H., Precise Gravimetric Geodesy, Dept. of Geodetic Science Report No. 219, The Ohio State University, Columbus, 1974.

Moritz, H., Integral Formulas and Collocation, Dept. of Geodetic Science Report No. 234, The Ohio State University, Columbus, 1975.

Moritz, H., Advanced Physical Geodesy, Wichmann Verlag, Karlsruhe, 1980.

Neyman, Y. M., Isotropy Conditions for a Probability Study of the Gravitational Field, Geodesy, Mapping & Photogrammetry, 16, 2, 71-74, 1974.

Neyman, Y.M., Probability Modification of Stokes Formula for Calculating the Height Anomaly, Geodesy, Mapping & Photogrammetry, 16, 3, 137-139, 1974.

Peucker, T.K., R.J. Fowler, J.J. Little, D.M. Mark, The Triangulated Irregular Network, Proc. Digital Terrain Models (DTM) Symposium, 516-540, St. Louis, 1978.

Rapp, R.H., Mean Gravity Anomalies and Sea Surface Heights Derived from GEOS-3 Altimeter Data, Dept. of Geodetic Science Report No. 268, The Ohio State University, Columbus, 1977.

Rapp, R.H., Ellipsoidal Corrections for Undulation Computations Using Gravity Anomalies in a Cap, Journal Geophysical Research, 86, B11, 10843-10848, 1981.

Rummel, R., R.H. Rapp, The Influence of the Atmosphere on Geoid and Potential Coefficient Determination from Gravity Data, Journal Geophysical Research, 81, 32, 5639-5642, 1976.

Rummel, R., L. Sjöberg, R.H. Rapp, The Determination of Gravity Anomalies from
   Geoid Heights, Dept. of Geodetic Science Report No. 269, The Ohio State
   University, Columbus, 1977.

Rummel, R., K.-P. Schwarz, M. Gerstl, Least Squares Collocation and Regulariza-
   tion, Bull. Geod., 53, 343-361, 1979.

Rummel, R., A Direct Method of Geoid Height Computation from Discrete Gravity
   Anomalies, paper pres. IAG General Meeting, Tokyo, 1982.

Shamos, M.I., D. Hoey, Closest Point Problems, Proc 16th Annual Symp. Foundations
   Computer Sciences, 151-162, 1975.

Sjöberg, L., Integral Formulas for Heterogeneous Data in Physical Geodesy,
   Bull. Geod., 53, 296-315, 1979.

Tscherning, C.C., R.H. Rapp, Closed Covariance Expressions for Gravity Anomalies,
   Geoid Undulations, and Deflections of the Vertical Implied by Anomaly
   Degree Variance Models, Dept. of Geodetic Science Report No. 208, The Ohio
   State University, Columbus, 1974.

Tscherning, C.C., Application of Collocation Determination of a Local Approx
   -imation to the Anomalous Potential of the Earth Using "Exact"-Astro-Grav-
   imetric Collocation, in Methoden und Verfahren der mathematischen Physik,
   Bd. 14/3, eds., Brosowski, B., E. Martensen, Bibliographisches Institut,
   83-110, Mannheim, 1975.

Wenzel, H.-G., Zur Geoidbestimmung durch Kombination von Schwereanomalien und
   einem Kugelfunktiousmodell mit Hilfe von Integralformeln, Zeitschrift für
   Vermessungswesen, 106,3,102-111, 1981.

## Appendix

The stabilized global estimator is obtained by considering the limit case of equation (9), where the observation points become globally dense, i.e. where one approaches a continuous coverage with observations all over the earth. This type of limit is explained in (Moritz, 1975, ch.2). The derivation of the limits is especially convenient, if one expresses all quantities in their spectral form. For then, as pointed out in chapter 2, the functions--or global limits-- can be represented as infinite dimensional vectors. The inner product $\{f , g\}_H$ in $H$ for example defined as

$$\{f , g\}_H = \frac{1}{4\pi} \int_\sigma f(P) \, g(P) \, d\sigma_P$$

becomes, when using the spectral forms,

$$\{f , g\}_H = \frac{1}{4\pi} \int_\sigma (\sum_{\ell m} f_{\ell m} \, Y_{\ell m}(P)) \, (\sum_{\ell' m'} g_{\ell' m'} \, Y_{\ell' m'}(P)) \, d\sigma_P$$

$$= \sum_{\ell m} f_{\ell m} \, g_{\ell m} ,$$

where the orthogonality relationships of spherical harmonics were used. In a first step, we shall now apply this principle to equations (10) and (11), where the outcome is known from the literature. The (isotropic) operator $S^{-1}$ can be written as

$$\underset{\infty \times n}{S^{-1}} = \sum_\ell (\frac{r_{Q'}}{r_{Q_i}})^{\ell+1} \lambda_\ell \, (2\ell+1) \, P_\ell \, (\cos\psi_{Q'Q_i})$$

$$= \sum_{\ell m} (\frac{r_{Q'}}{r_{Q_i}})^{\ell+1} \lambda_\ell \, Y_{\ell m}(Q') \, Y_{\ell m}(Q_i) \qquad i=1,\dots n, \qquad (A-1)$$

where the addition theorem was used:

$$P_\ell(\cos\psi_{Q'Q}) = \frac{1}{2\ell+1} \sum_m Y_{\ell m}(Q') \, Y_{\ell m}(Q) . \qquad (A-2)$$

Applying the principle shown above we find with eq. (4) for eq. (10):

$$\underset{\infty \times n}{C_{tg}} = \underset{\infty \times \infty}{C_{tt}} \; \underset{\infty \times n}{S^{-T}} =$$

$$= \frac{1}{4\pi} \int_\sigma [ \sum_{\ell m} (\frac{R^2}{r_P r_{Q'}})^{\ell+1} \frac{c_\ell}{2\ell+1} \, Y_{\ell m}(P) \, Y_{\ell m}(Q')] \cdot$$

$$\cdot [ \sum_{\ell' m'} (\frac{r_{Q'}}{r_{Q_i}})^{\ell'+1} \lambda_{\ell'} \, Y_{\ell' m'}(Q') \, Y_{\ell' m'}(Q_i)] \, d\sigma_{Q'}$$

$$= \sum_{\ell m} (\frac{R^2}{r_P r_{Q_i}})^{\ell+1} \lambda_\ell \frac{c_\ell}{2\ell+1} \, Y_{\ell m}(P) \, Y_{\ell m}(Q_i) \quad \text{and} \quad i=1,\dots n. \qquad (A-3)$$

-29-

Furtheron, for equation (11) one obtains:

$$\underset{n \times n}{\underline{C}_{gg}} = \underset{n \times \infty}{\underline{S}^{-1}} \; \underset{\infty \times \infty}{\underline{C}_{tt}} \; \underset{\infty \times n}{\underline{S}^{-T}}$$

$$= \frac{1}{4\pi} \int_\sigma \left[ \sum_{\ell' m'} \left(\frac{r_P}{r_{Q_j}}\right)^{\ell'+1} \lambda_{\ell'} \; \overline{Y}_{\ell' m'}(Q_j) \; \overline{Y}_{\ell' m'}(P) \right] \cdot$$

$$\cdot \left[ \sum_{\ell m} \left(\frac{R^2}{r_P r_{Q_i}}\right)^{\ell+1} \lambda_\ell \; \frac{c_i}{2\ell+1} \; \overline{Y}_{\ell m}(P) \; \overline{Y}_{\ell m}(Q_i) \right] d\sigma_P$$

$$= \sum_{\ell m} \left(\frac{R^2}{r_{Q_j} r_{Q_i}}\right)^{\ell+1} \lambda_\ell^2 \; \frac{c_\ell}{2\ell+1} \; \overline{Y}_{\ell m}(Q_j) \; \overline{Y}_{\ell m}(Q_i) \quad \text{and} \quad i,j = 1,\ldots n \qquad \text{(A-4)}$$

Now to the global limit, which we denote $\lim(Q_i$ globally dense on $\sigma_Q)$ or short $\underset{Q_i \text{dense}}{\lim}$ . In case random, uncorrelated measurement noise with variance $\sigma_\delta^2$ is assumed the global limit of the a priori variance-covariance matrix $\underline{D}$ can be expressed as

$$\underset{Q_i \text{dense}}{\lim} \; \underline{D} = \underset{\infty \times \infty}{\underline{D}} = \sigma_\delta^2 \sum_{\ell m} \overline{Y}_{\ell m}(P) \; \overline{Y}_{\ell m}(Q) , \qquad \text{(A-5)}$$

compare (Heiskanen & Moritz, 1967, ch. 7-7). It is in principle a critical. point, because several severe statistical assumptions enter this derivation. We try a short derivation. Let us assume the a priori model of the uncorrelated noise is expressable by the random function $\tilde{\epsilon}(P)$ . Its covariance function is

$$D(P,Q) = \sigma_\delta^2 \; \delta(P,Q) \qquad \text{(A-6)}$$

with the delta function

$$\delta(P,Q) = \begin{cases} \infty \text{ for } P = Q \\ \\ 0 \text{ for } P \neq Q \end{cases} \quad \text{and } P,Q \in \sigma$$

The spectral components of $D(P,Q)$ (power spectrum components, in the time-series terminology) are obtained from:

$$d_{\ell m} = \frac{1}{16\pi^2} \int_\sigma \int_{\sigma'} D(P,Q) \; \overline{Y}_{\ell m}(PQ) \; \overline{Y}_{\ell m}(Q) \; d\sigma_P \; d\sigma'_Q$$

$$= \sigma_\delta^2 \frac{1}{4\pi} \int_\sigma \delta(P,P) \; \overline{Y}_{\ell m}^2(P) \; d\sigma_P \qquad \text{(A-7)}$$

The mathematical distribution, $\delta(P,Q)$, is defined in such a way that

$$\frac{1}{4\pi} \int_\sigma \delta(P,P) \, \bar{Y}_{\ell m}^2 (P) \, d\sigma_p \overset{def.}{=} 1 \tag{A-8}$$

Thus, one obtains from equation (A-7)

$$d_{\ell m} = d = \sigma_\delta^2 . \tag{A-9}$$

For the finite case with one sample point per $\Delta s = \sin \phi \Delta\phi\Delta\lambda$ on the unit sphere $\sigma$, Jekeli and Rapp (1980) derived the approximation to equation (A-9):

$$d' = \frac{\Delta s}{4\pi} \, \sigma_\delta^2 . \tag{A-10}$$

With equations (A-4) and (A-9) the global limit of $(\underline{S}^{-1}\underline{C}_{tt}\underline{S}^{-T}+\alpha\underline{D})$, compare equation equation (9), becomes

$$\lim_{Q_i \text{dense}} (\underline{S}^{-1}\underline{C}_{tt} \, \underline{S}^{-T} + \alpha\underline{D}) =$$

$$= \sum_{\ell m} [(\frac{R^2}{r_Q^2})^{\ell+1} \lambda_\ell^2 \, \bar{\bar{c}}_\ell + \alpha\sigma_\delta^2] \, \bar{Y}_{\ell m}(Q) \, \bar{Y}_{\ell m}(Q') \tag{A-11}$$

where

$$\bar{\bar{c}}_\ell \overset{def.}{=} \frac{c_\ell}{2\ell+1} \tag{A-12}$$

The inverse is

$$\lim_{Q_i \text{dense}} (\underline{S}^{-1}\underline{C}_{tt} \, \underline{S}^{-T} + \alpha\underline{D})^{-1} =$$

$$= \sum_{\ell m} [(\frac{R^2}{r_Q^2})^{\ell+1} \lambda_\ell^2 \, \bar{\bar{c}}_\ell + \alpha\sigma_\delta^2]^{-1} \, \bar{Y}_{\ell m}(Q) \, \bar{Y}_{\ell m}(Q') . \tag{A-13}$$

Finally, we obtain for the global limit of the complete estimator with equation (A-3):

$$\lim_{Q_i \text{dense}} \underline{C}_{tt} \, \underline{S}^{-T} (\underline{S}^{-1}\underline{C}_{tt} \, \underline{S}^{-T} + \alpha\underline{D})^{-1} =$$

$$= \frac{1}{4\pi} \int_\sigma [\sum_{\ell'm'} (\frac{R^2}{r_p r_Q})^{\ell'+1} \lambda_{\ell'} \, \bar{\bar{c}}_{\ell'} \, \bar{Y}_{\ell'm'} (P) \, \bar{Y}_{\ell'm'} (Q')] \cdot$$

$$\cdot [\sum_{\ell m} [(\frac{R^2}{r_Q^2})^{\ell+1}\lambda_\ell^2 \, \bar{\bar{c}}_\ell + \alpha\sigma_\delta^2]^{-1} \, \bar{Y}_{\ell m}(Q') \, \bar{Y}_{\ell m}(Q)] \, d\sigma_Q .$$

$$= \sum_{\ell m} \frac{(\frac{R^2}{r_p r_Q})^{\ell+1} \lambda_\ell \bar{\bar{c}}_\ell}{(\frac{R^2}{r_Q^2})^{\ell+1}\lambda_\ell^2 \bar{\bar{c}}_\ell + \alpha\sigma_\delta^2} \bar{Y}_m(P) \, \bar{Y}_m(Q) =$$

$$= \sum_{\ell m} \frac{(\frac{R^2}{r_Q^2})^{\ell+1} \lambda_\ell^2 \ \bar{\bar{c}}_\ell}{(\frac{R^2}{r_Q^2})^{\ell+1} \lambda_\ell^2 \bar{\bar{c}}_\ell + \alpha \sigma_\delta^2} \ (\frac{r_Q}{r_P})^{\ell+1} \ \frac{1}{\lambda_\ell} \ \bar{\Psi}_{\ell m}(P) \ \bar{\Psi}_{\ell m}(Q) \qquad\qquad (A\text{-}14)$$

-32-

# END

# FILMED

2-83

# DTIC